

## The Use of an Improved SCIT Algorithm to Investigate Lightning Characteristics of Several Severe Weather Episodes in North Georgia

John M. Trostel\* and Jenny Matthews  
Severe Storms Research Center, Georgia Tech Research Institute  
Atlanta Georgia

### 1 INTRODUCTION

The Severe Storms Research Center (SSRC) at the Georgia Tech Research Institute (GTRI) has developed an improved Storm Cell Identification and Tracking (SCIT) algorithm based on DBSCAN clustering and JPDA tracking. This improved algorithm has been used to associate National Lightning Detection Network (NLDN) cloud to ground (CG) and cloud to cloud (CC) lightning data with individual storm cells during a two tornado episodes which occurred in north Georgia on March 14 and 15, 2008. On the night of March 14<sup>th</sup>, an EF2 tornado transited downtown Atlanta, causing a fatality and considerable property damage. The next day, March 15<sup>th</sup>, saw three tornadoes which affected north Georgia, including an EF3 tornado which caused an additional two fatalities.

Earlier versions of a storm cell tracking algorithm developed by GTRI were based on the original SCIT algorithm used by the National Weather Service. Several improvements were initially made to the standard SCIT algorithm to better allow the association of distributed data, such as NLDN flash coordinates, with individually detected storm cells, as well as to track those cells in time. This early GTRI-modified SCIT algorithm was used to associate NLDN lightning data with the discrete supercells which transited the Atlanta, Georgia metropolitan area on March 14<sup>th</sup> 2008. These algorithms and the results obtained have been described in more detail in earlier work [*Trostel, 2008*].

An improved storm cell identification and tracking algorithm has been developed using DBSCAN (Density Based Spatial Clustering with Applications in Noise) clustering and JPDA (Joint Probabilistic Data Association) tracking methods. The DBSCAN clustering algorithm has proven to be much more robust than earlier methods in areas of non-uniform reflectivity. The JPDA tracking method has proven to be reliable in cluttered reflectivity environments, such as those found in the March 15<sup>th</sup> tornado episode. The details of the new algorithms are described in a companion paper [*Matthews and Trostel, 2010*]. These improved methods were used to associate NLDN data with individual cells embedded in the more complex mesoscale systems seen on March 15<sup>th</sup>. The use of these tracking and association algorithms allowed the type of lightning (CG vs. IC), as well as stroke polarity to be examined as a function of cell evolution and strength.

---

\* Corresponding author address: John M. Trostel, Severe Storms Research Center, Georgia Tech Research Institute, Georgia Institute of Technology, Atlanta, GA 30332-0857; email: john.trostel@gtri.gatech.edu

Various trends in lightning rates, including jumps in flash rate preceding tornadoes and decreases in flash rate during touchdown were noted for both days. Lightning jumps have been previously associated with the onset of severe weather [Williams *et al.*, 1999] and various lightning jump algorithms have been developed to aid in the forecasting of severe weather often associated with thunderstorms [Schultz *et al.*, 2009].

## **2 DATA SOURCES**

### **2.1 NEXRAD Radar Data**

NEXRAD radar data from the Peachtree City NWS was collected from the level II archives at NCDC for both March 14<sup>th</sup> and March 15<sup>th</sup> 2008. These data sets were then run through the WDSS-II [Lakshmanan, Smith, *et al.*, 2007] quality control algorithms [Lakshmanan, Fritz, *et al.*, 2007] The WDSS-II program was used to initially overlay the NLDN flash data with the reflectivity data to ensure that cell association was possible, as well as to gain a basic overview of the storms. The quality controlled NEXRAD data was then ingested, along with NLDN lightning data, into either the early GTRI-modified routines or the recently developed DBSCAN routines.

### **2.2 NLDN Lightning Data**

Both Cloud to Ground (CG) and Cloud to Cloud (CC) lightning flash and stroke data was acquired from Vaisala's National Lightning Detection Network (NLDN) for the state of Georgia covering the days of March 14<sup>th</sup> and 15<sup>th</sup>, 2008. The NLDN consists of over 100 remote, ground-based "IMPACT" sensors broadly distributed over the continental United States. These sensors collaboratively detect the location of lightning events using both direction finding (DF) and time of arrival (TOA) methods. Typically between 6 and 8 sensors are used to detect each event.

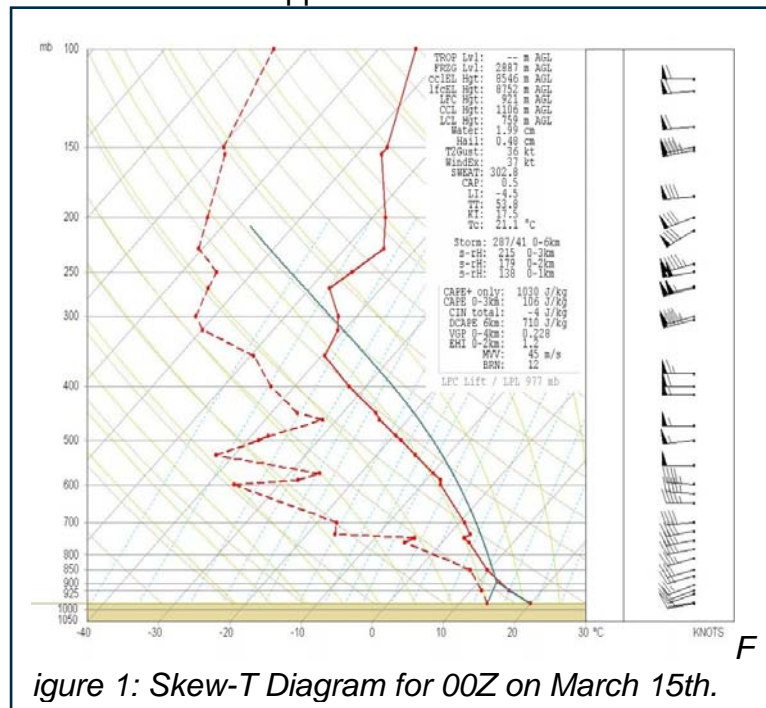
The data from each IMPACT sensor is collected at the National Collection Center (NCC) located in Tucson, Arizona. At the NCC, the data is analyzed to produce data sets consisting of stroke location, time, polarity, amplitude and type. Additionally, strokes are grouped into flashes based on temporal and spatial constraints. CG flash detection efficiency with the NLDN approaches 95 percent, with a median location accuracy of 500 meters. CC events, typically one or two per flash, are detected at a lower efficiency, on the order of 10 to 20 percent.

## **3 MARCH 14<sup>TH</sup> SUPERCELLS**

### **3.1 Synoptic Overview for March 14<sup>th</sup>**

Figure 1 displays the Peachtree City, Georgia WFO (KFFC) sounding at 00Z from March 15, 2008. Peachtree City is located about 30 miles south of the metropolitan Atlanta area, where the tornado touched down. The 00Z sounding corresponds to a local time of 8:00pm, about 90 minutes prior to the touchdown at 9:38pm. The sounding

indicated a modest CAPE value of 1030 J/kg. The 0-3 km SRH values were found to be relatively high at  $215 \text{ m}^2/\text{s}^2$ . This situation was characteristic of a cool season storm development with the low, modest CAPE values coupled with the high SRH values. The wind values plotted on the sounding indicate a highly sheared environment, although the shear is almost entirely speed shear at the time of the sounding. The KFFC sounding displayed westerly winds throughout the vertical with only changes in wind speeds. These changes were, however, dramatic, with the speed increasing from 30-40 kts in the low levels to over 100 kts at upper levels.



The March 14<sup>th</sup> 12Z (8am local time) and March 15<sup>th</sup> 00Z (8pm local time) surface charts as seen in Figure 2 and Figure 3, respectively, set up the surface synoptic situation just prior to the tornado touchdown. A large low pressure system initially located in the Arkansas – Tennessee area at 12Z, in Figure 1, has moved into the Virginia area by 00Z trailing a cold front.

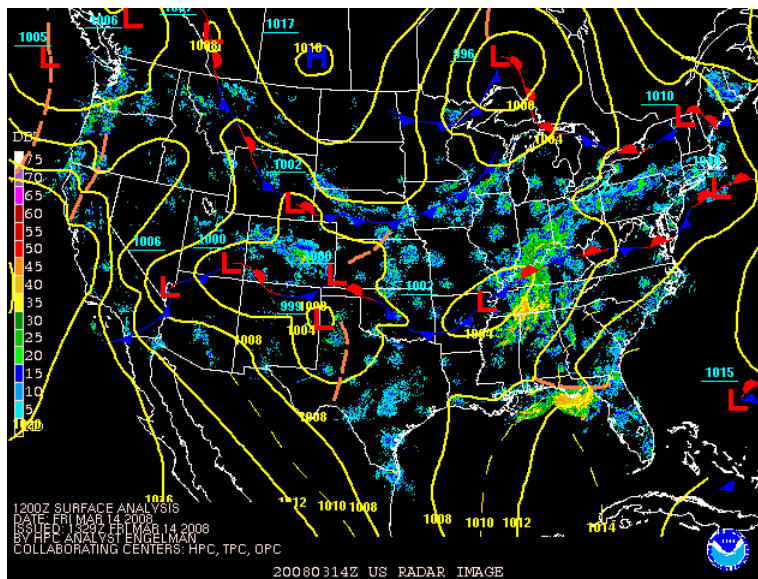


Figure 2: Surface Chart at 12Z on March 14th

Careful examination of the March 15<sup>th</sup> 00Z chart in Figure 3 shows two supercells starting to form in eastern Alabama and western Georgia just ahead of the cold front. The first supercell produced the EF2 tornado that would affect metropolitan Atlanta.

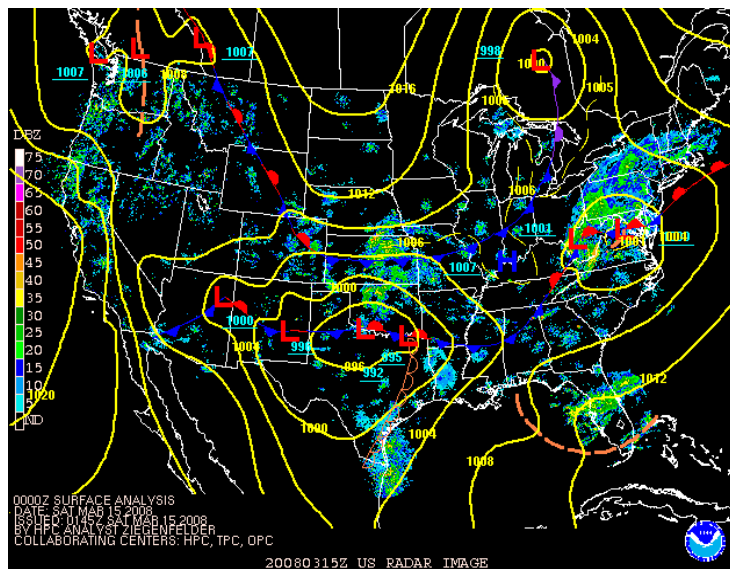


Figure 3: Surface Chart at 00Z on March 15th.

### 3.2 March 14<sup>th</sup> Results

Preliminary analysis of the March 14<sup>th</sup> storms involved ingestion of the Level-II NEXRAD data into the WDSS-II processing system. NLDN data sets were also input into WDSS-II and aligned in time and space with the radar data. Figure 4 shows the KFFC composite reflectivity data along with the corresponding NLDN data for 03Z on March 15<sup>th</sup>. This is about 90 minutes after the EF2 tornado had hit downtown Atlanta.

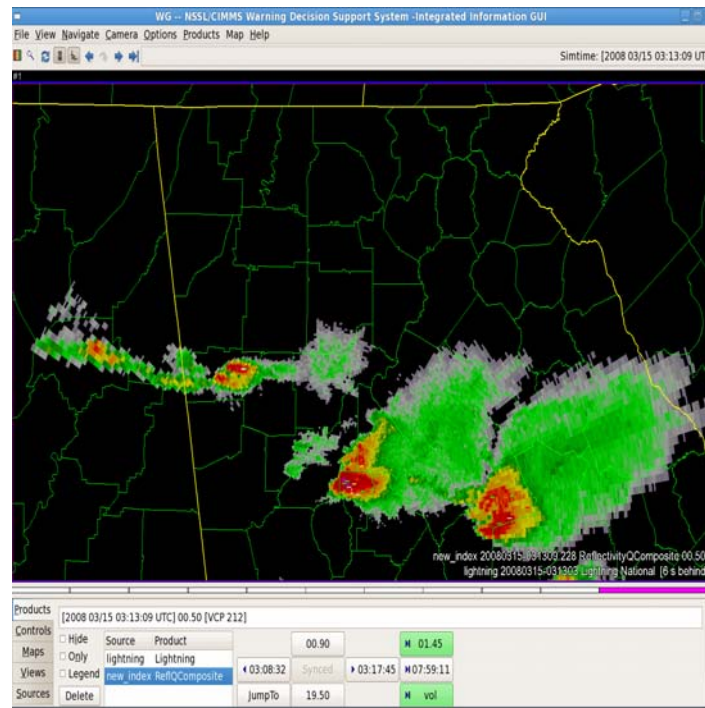
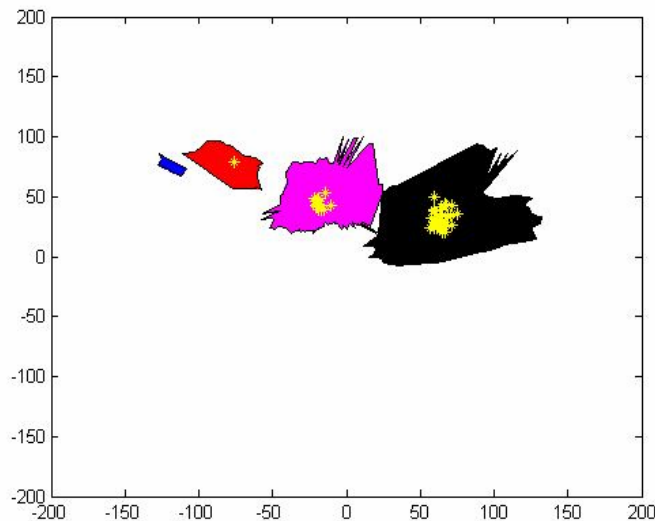


Figure 4: NEXRAD and NLDN flash data for 03Z on March 15<sup>th</sup>

The tornadic supercell is the farthest east of the two large supercells shown in central Georgia. The NLDN data assimilated with the WDSS-II composite reflectivity output is depicted in this plot as '+' and '-' symbols, showing the locations of positive and negative flashes respectively. These two supercells, along with the smaller cell just past the western border of Georgia were examined using the early GTRI algorithms.

An example frame of the processed output using the early GTRI-modified SCITs and the associated NLDN data is shown in Figure 5. The two large supercells are colored black (tornadic) and magenta (non-tornadic), while the smaller trailing cell is colored red. The NLDN flash data points are depicted as yellow '\*' signs and can be seen to be well associated with each storm cell.



*Figure 5: Original SCIT processing and associated NLDN flashes for March 14th storms.*

The association of individual NLDN flashes with each cell allowed the lightning characteristics of the cells to be examined as a function of cell type and lifetime. Figure 6 shows the total (CC + CG) flash rate for each cell as a function of radar scan number. The flash rate for the main EF2 bearing cell is shown in green, the rate for the non-tornadic cell is shown in blue, and the rate for the third, smaller trailing cell is shown in red. The period when the EF2 tornado was reported on the ground is depicted as an inverted black triangle just above the green, EF2 cell trace at scan 21.

The total flash rate for the tornadic cell starts at a reasonably high level (the cells are only tracked within the state of Georgia), but then decreases dramatically right before tornado touchdown. After touchdown, the EF2 cell total flash rate again increases and reaches levels higher than those seen before the tornado. The flash rates for the second, non-tornadic cell show some jumps and decreases, but never reaches the levels seen in the tornadic storm. The third, small cell shows much lower overall rates than either of the large supercells. It should be noted that some of these differences may be due to changing cell area; a factor not addressed in the early GTRI-modified SCIT algorithms.

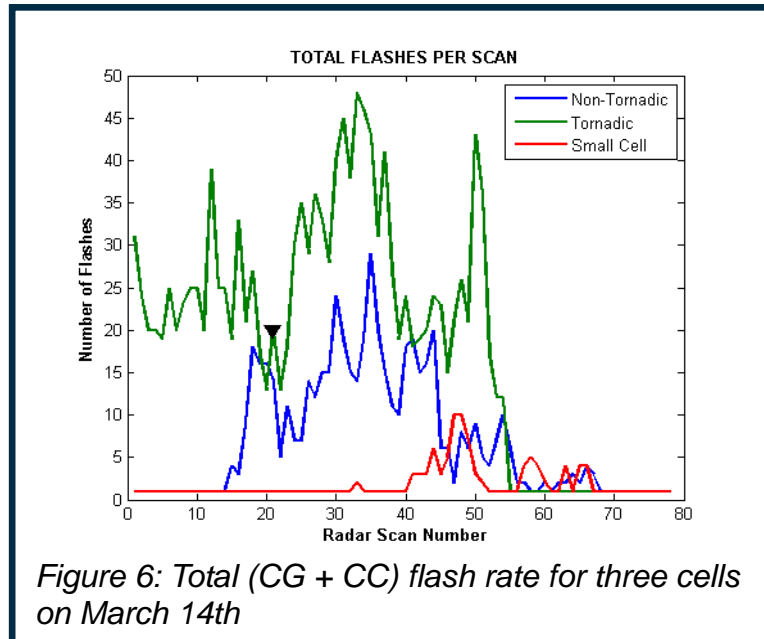


Figure 6: Total (CG + CC) flash rate for three cells on March 14th

The CG flash rates for each cell, shown in Figure 7, do not show much difference between the two supercells. Both the tornadic and non-tornadic supercells show relatively persistent rates over the lifetime of the cells. Again, the small cell shows dramatically lower flash rates, likely due to that cells much smaller size and strength.

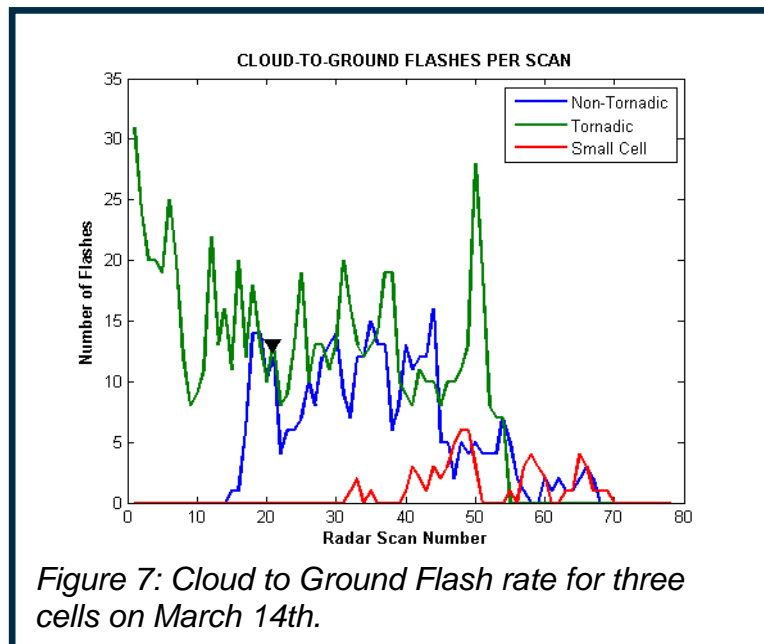
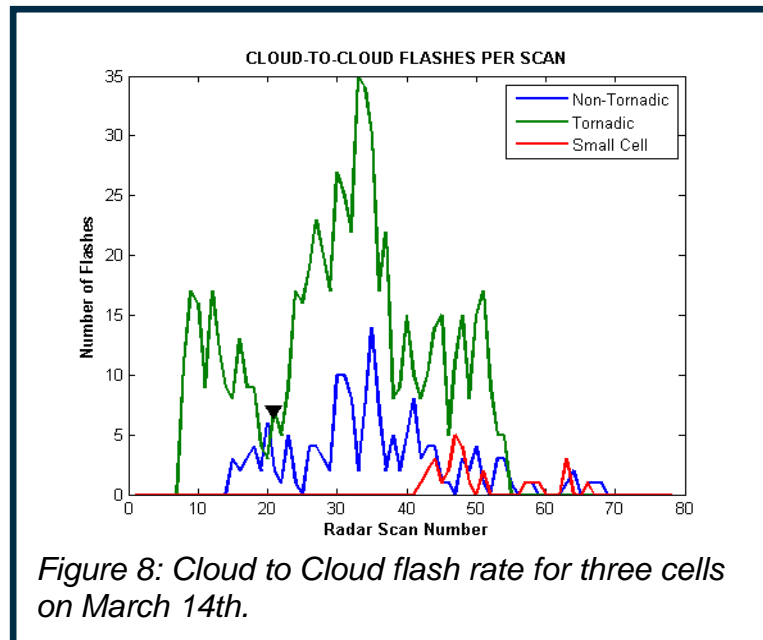


Figure 7: Cloud to Ground Flash rate for three cells on March 14th.



The CC flash rate for the three cells, shown in Figure 8, is somewhat more interesting. As was the case with the total flash rate, the tornadic supercell shows higher rates overall than either of the other cells. It also shows a drop coincident with tornado touchdown and a subsequent increase. The CC rate for the non-tornadic supercell is generally much lower and does not present such a dramatic drop (or jump) during its history.



Again, the small trailing cell shows much lower flash rates than either supercell.

## 4 MARCH 15<sup>TH</sup> OUTBREAK

### 4.1 Synoptic Summary for March 15th

A severe weather outbreak occurred during the day and into the evening of March 15<sup>th</sup> 2008. SPC storm reports, reproduced in Figure 9, show an area of tornadoes, hail, and high winds stretching from northeast Alabama, through northern Georgia, and into South Carolina. Three of these tornadic storms were quickly verified by the NWS and have been subjected to analysis using the improved DBSCAN SCIT algorithms with JPDA cell tracking.



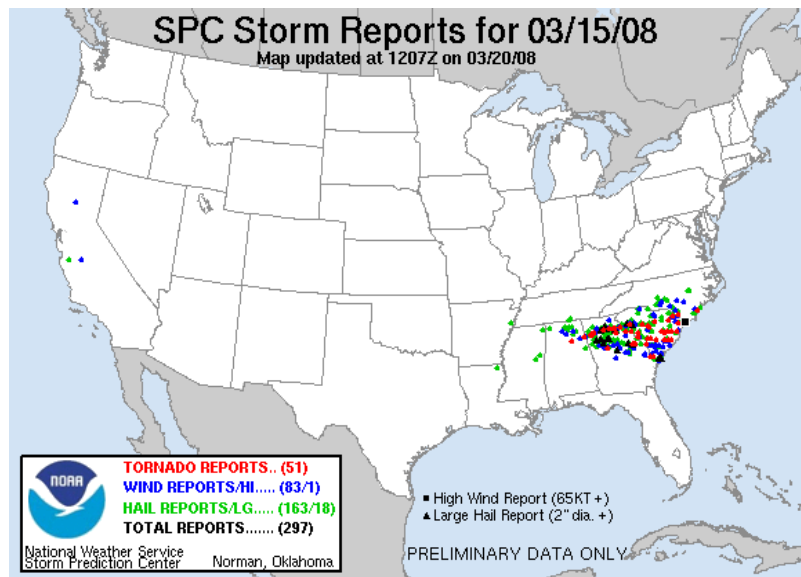


Figure 9: Storm Reports for March 15 2008 Outbreak

The surface synoptic chart, Figure 10, for 15Z (11 AM local time) on March 15<sup>th</sup> shows an occluded front sagging across northern Georgia. The first, EF3 tornadic cell formed along this boundary about 90 minutes later at 1625Z.

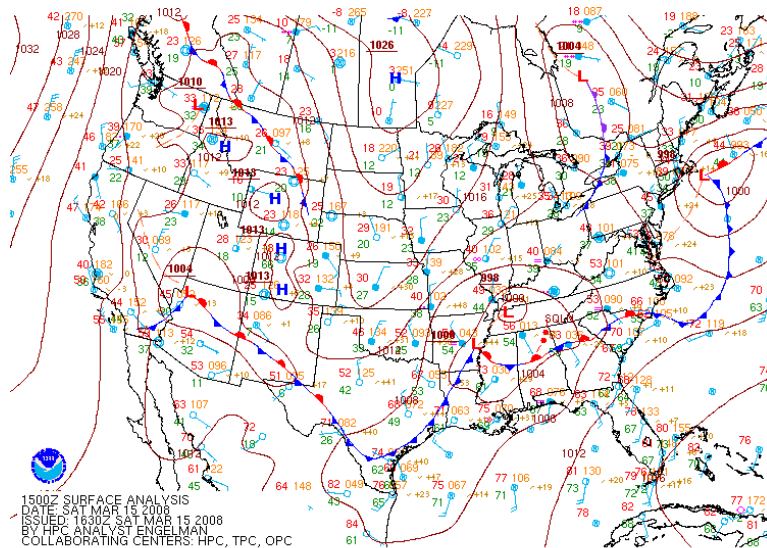
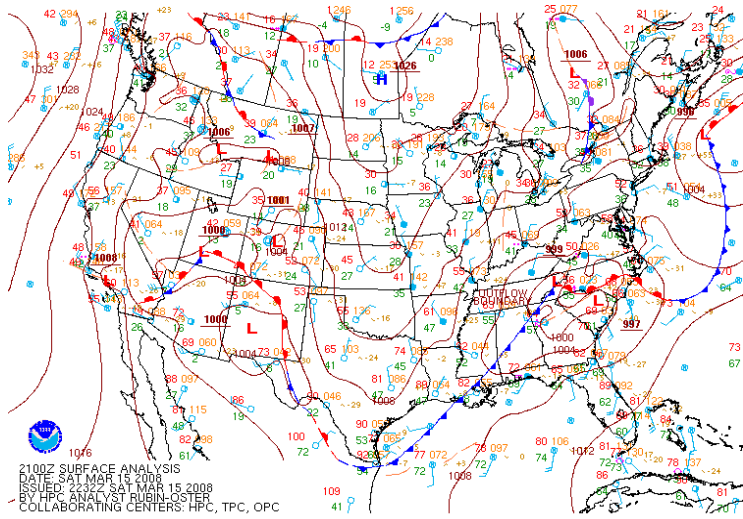


Figure 10: Surface Chart for 15Z on March 15th.

By 21Z (5 PM local time) the surface chart, Figure 11, showed the surface low that had been in western Tennessee having moved to the Tennessee / North Carolina border, drawing a cold front behind it into northwest Georgia. A second string of severe

thunderstorm cells formed ahead of this front, with two tornadoes reported at 2215Z (6:15 PM local time).

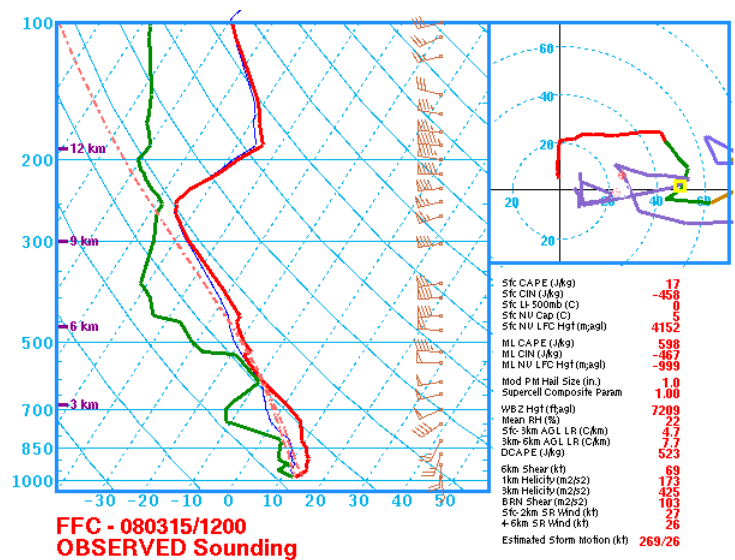


2100Z SURFACE ANALYSIS  
DATE: SAT MAR 15 2008  
TIME: 2100Z SAT MAR 15 2008  
BY: HPC ANALYST RUDINOSTER  
COLLABORATING CENTERS: HPC, TPC, OPC

Fi

Figure 11: Surface Chart at 21Z on March 15th.

A sounding from KFFC at 12Z, presented in Figure 12, on the 15<sup>th</sup> shows only modest CAPE values ( $598 \text{ Jkg}^{-1}$ ) accompanied by 0-3km SRH values of  $425 \text{ m}^2\text{s}^{-2}$ . Considerable speed shear is evident in the lower part of the sounding.



FCC - 080315/1200  
OBSERVED Sounding

NHUSNCEPISPC

Figure 12: Skew-T Diagram for 12Z on March 15th.



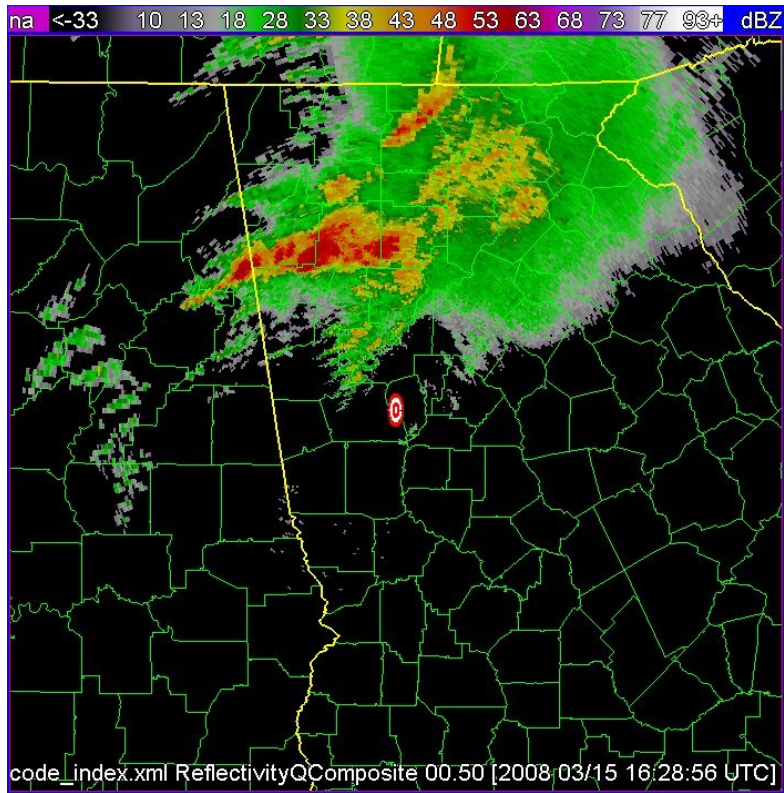


Figure 14 NEXRAD Image from 1629Z March 15<sup>th</sup>

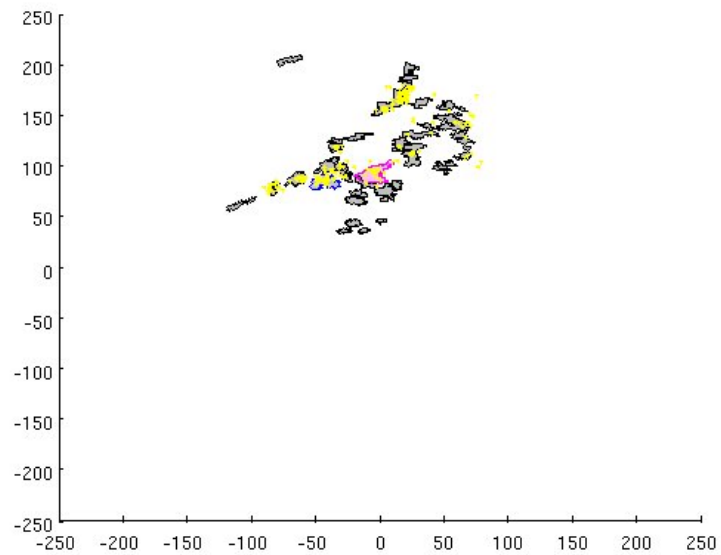


Figure 15 DBSCAN SCITs and NLDN Flashes at 1625Z on March 15<sup>th</sup>

The magenta cell shown in Figure 15 is a non-tornadic cell contained in the MCS. Just to the left of that cell, the cell containing the EF2 tornado is colored blue. The NLDN data points are shown as yellow '\*' symbols plotted on top of the detected DBSCAN cells. Many other cells, which were not analyzed for this effort, are shown colored in gray.

Figure 16 shows the NEXRAD composite reflectivity image which corresponds a period later in the day when tornadic storms were forming ahead of the trailing cold front in northwest Georgia. The storms formed in the line of storms shown across central Georgia, just to the right of the red and white "bullseye", which shows the location of the KFFC NEXRAD facility. An EF2 and an EF0 tornado were reported on the ground at 2215Z (6:15 PM local), the time this radar image was made. Figure 17 shows the corresponding DBSCAN and NLDN data.

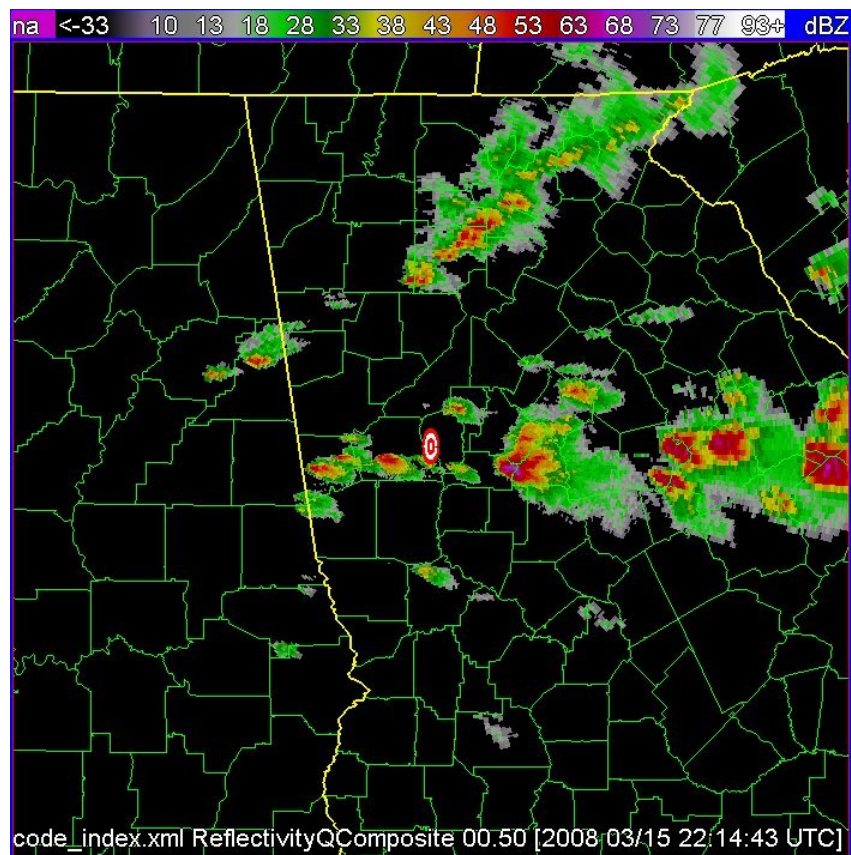
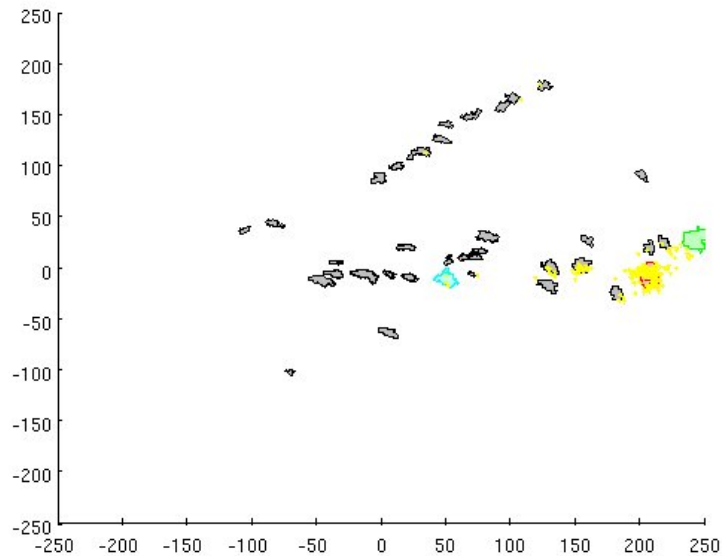


Figure 16 NEXRAD composite reflectivity at 22:15 UTC on March 15<sup>th</sup>





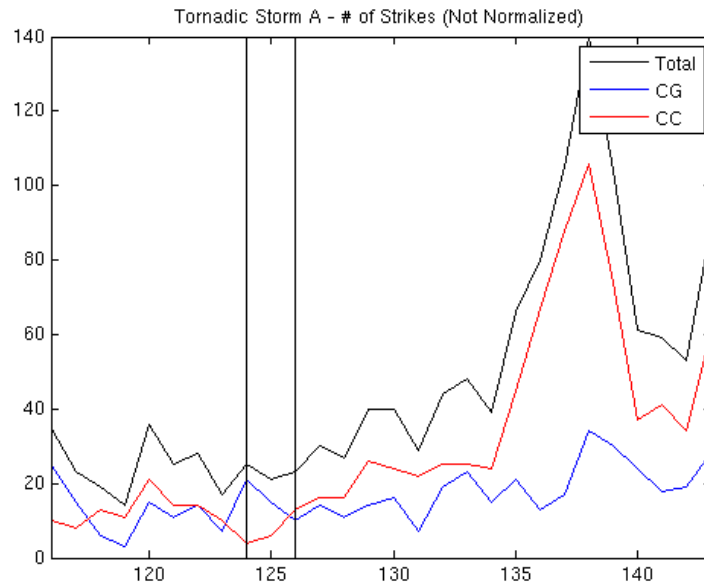
*Figure 17 DBSCAN SCITs and Associated NLDN Flashes*

A storm cell containing the EF2 tornado is plotted on Figure 17 in red, but is hard to see under a sea of NLDN flash data near the right side of the figure. Just to the right of the EF2 cell, a non-tornadic cell, which was also tracked and analyzed, is colored in green. The cyan cell containing the small, EF0 tornado is nearly in the middle of the plot.

### **4.3 Flash Rates for March 15<sup>th</sup> Storms**

Flash rates for the storm cells examined in the March 15<sup>th</sup> outbreak were also separated into CC flashes, CG flashes, positive flashes and negative flashes. In an improvement to the processing produced for the March 14<sup>th</sup> supercells, the flash rates were normalized with respect to the ground area covered by the DBSCAN SCIT. The effect of this normalization is demonstrated below in Figure 18, showing the unnormalized total (CC+CG), CC, and CG flash rates for the first EF3 tornadic cell, and Figure 19, which shows the same data after normalization.

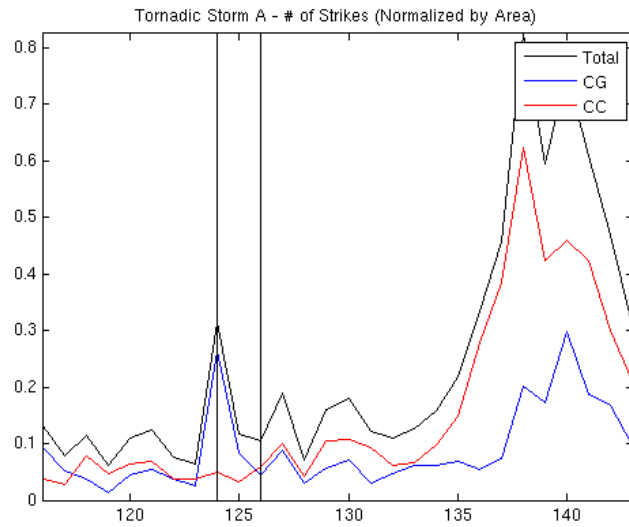
Figure 18 shows the total number of strikes detected during each NEXRAD scan interval along the y-axis. The numbers along the x-axis denote the NEXRAD radar scan, one approximately every 5 minutes, used to correlate the reflectivity data to the lightning data. The black line shows the total number flashes (CC + CG) detected, while the red and blue lines depict the number of CC and CG flashes detected respectively. The thick black line parallel to and below the x-axis from NEXRAD scan 124 to scan 131 indicates the period when the tornado was reported to be on the ground. In this figure there is no apparent jump in lightning rate prior to tornado touchdown.



*Figure 18 Total flashes (CC + CG) for EF3 tornadoic storm without area normalization*

In Figure 19, the same basic data is used. Now the effects of normalization are shown as an increase in area normalized flash rates just prior to tornado touchdown. The y-axis in this plot is now normalized to flashes  $\text{km}^{-2}$  during each NEXRAD scan interval. This allows a modest, short-lived jump in the area adjusted flash rate to be seen just prior to tornado touchdown. This increase is solely for CG flashes and occurs only at most one NEXRAD scan interval (about 5 minutes) before touchdown. After the tornado has lifted, the cell shows a later, similar increase in CG flash rate that accompanies a much larger increase in CC flash rate.

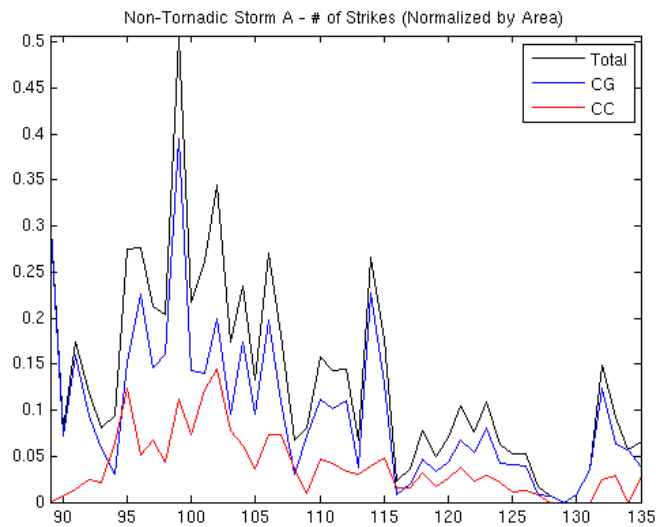




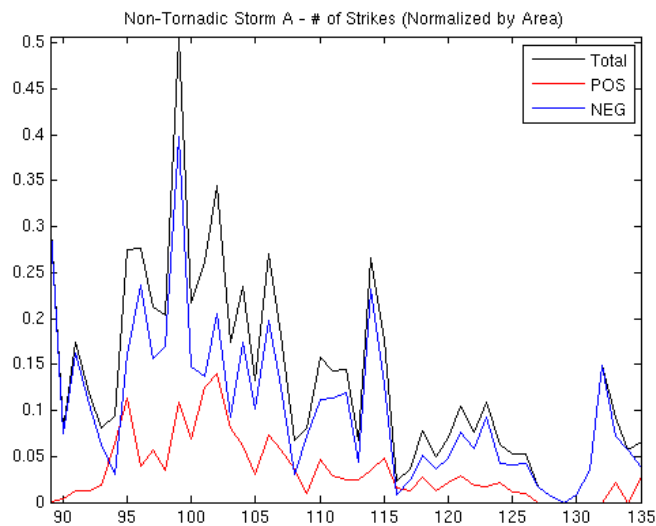
*Figure 19 Total Flashes (CC+CG) for EF3 Cell with area normalizarion*

The area-normalized CC and CG flash rates for the non-tornadoic partner cell to the EF3 tornadoic cell are shown in Figure 20, while the positive to negative flash rates for this non-tornadoic storm are shown in Figure 21. The non-tornadoic partner cell to the EF3 tornadoic cell showed some periods when the normalized flash rate was comparable to the EF3 storm. There are also several periods of fairly intense flash rates and subsequent periods of low rates. In all cases for this non-tornadoic storm, however, the CC and positive flash rates were consistently lower than the CG and negative rates.





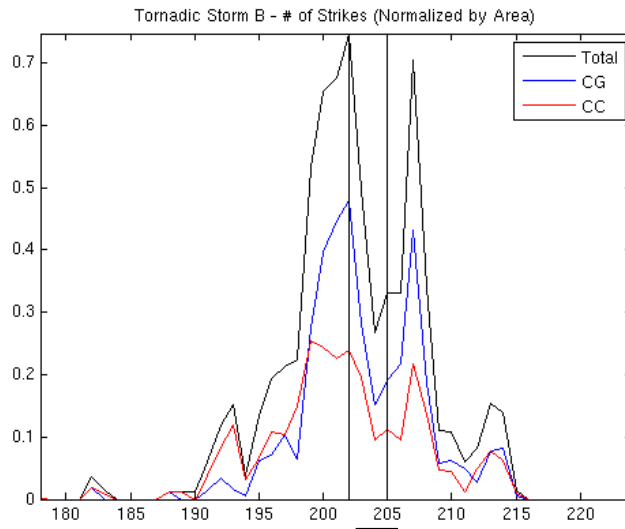
*Figure 20: Normalized CC and CG Flash Rates for first non-tornadic cell on March 15th*



*Figure21: Normalized Positive and Negative flash rates for first non-tornadic cell studied on March 15th.*

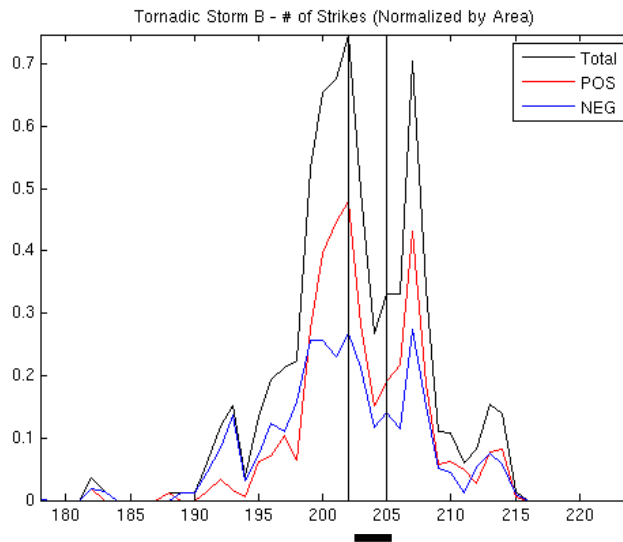
The three cells which formed later in the day in the line of storms ahead of the advancing cold front during the evening on March 15<sup>th</sup> were also examined using the DBSCAN SCIT algorithm. These included an EF2 tornadic cell, a second accompanying non-tornadic cell and a third, small EF0 tornadic cell.

The area normalized CG and CC flash rates for the EF2 cell are shown in Figure 22, and may be compared to the normalized positive and negative flash rates for the same storm shown in Figure 23.



*Figure22: CC and CG flash rates for the EF2 tornadic cell on March 15th*

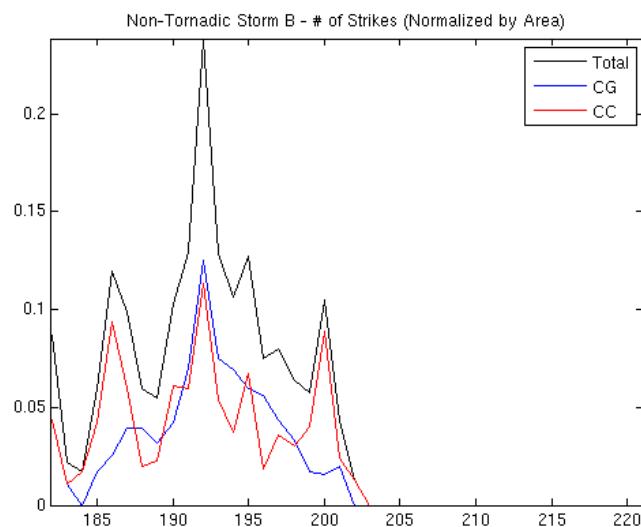
Again, in these plots, the period when the tornado was reported to be on the ground is depicted by a black line along the horizontal, x-axis of the plots, corresponding to NEXRAD scans 202 through 205. Both the CG and the CC rates, as well as the positive and negative rates, show large increases prior to touchdown and a significant reduction during the period the tornado was reported on the ground.



*Figure 23: Positive and negative flash rates for the EF2 tornadoic cell on March 15th.*

Comparing Figure 22 to Figure 23 shows that, in this cell, the CG strokes during the lightning jump were primarily positive. It should also be noted that the flash rate for this cell was nearly twice as high as that seen for the preceding EF3 tornadoic cell.

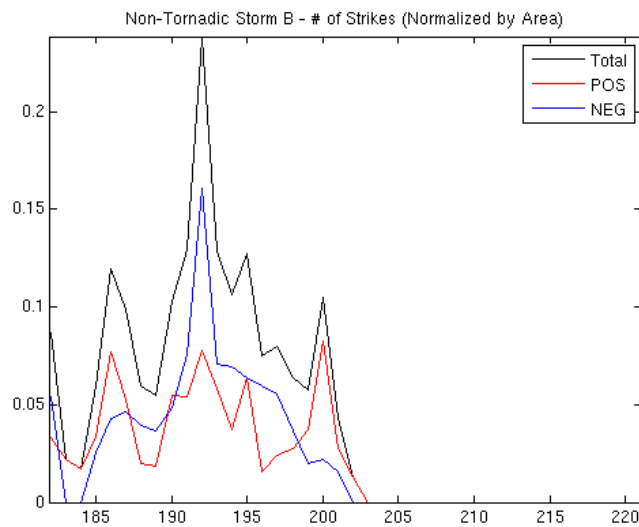
One of the cells training in the line in front of the approaching cold front that did not produce a tornado was also studied for comparison. The normalized flash rates calculated for this cell are presented in Figures 24 and 25.



*Figure 24: CC and CG flash rates in non-tornadoic storm in latter part of March 15th outbreak.*

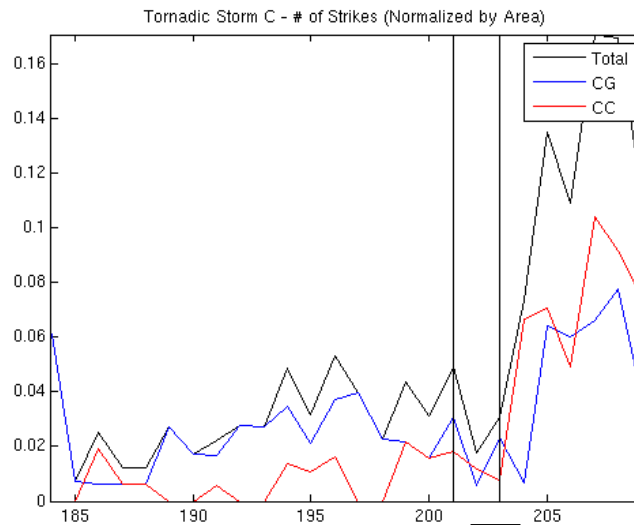
Although the storm started with periods when the CC flashes outnumbered the CG flashes, during the most vigorous part of the storm, the CG and CC rates were nearly equal.

Figure 25 also shows that, while positive flashes were common in the beginning and ending of the cell lifetime, negative flashes dominated in this non-tornadic cell during the most vigorous part of the storm. It should also be noted that the peak of the lightning jump seen in this cell is much lower than that seen in the EF2 cell, reaching only about  $0.25 \text{ strikes km}^{-2} \text{ scan}^{-1}$ .



*Figure 25: Positive and negative flash rates for non-tornadic cell in latter part of March 15th outbreak.*

The final cell studied in this effort was a small EF0 tornadic storm that formed about the same time as the EF2 tornado bearing cell. The lightning characteristics of the EF0 cell are shown in Figure 26.



*Figure26: CC and CG flash rates for a small EF0 tornadic cell on March 15th.*

The peak flash rates in this cell were never as high as the rates seen in any of the other cells. Although a small decrease in flash rate is seen after tornado touchdown, the major increase in flash rate appears after the small tornado has lifted.

## 5 CONCLUSIONS

The storms seen near Atlanta on March 14<sup>th</sup> and 15<sup>th</sup> of 2008 were typical of a cool-season tornadic scenario for Georgia. The storms seen during the night of March 14<sup>th</sup> were late evening, low topped supercells. Cells on March 15<sup>th</sup> included embedded cells in the mid-morning set of storms and small isolated cells later in the day. The environment was characterized by only modest CAPES near 1000 Jkg<sup>-1</sup> and high shears, with the 3 km SRH between 191 and 425 m<sup>2</sup>s<sup>-2</sup>.

Improvements have been made in the storm cell tracking and association algorithms used to study these storms. The more simplistic methods used successfully for the March 14<sup>th</sup> storms have been improved to provide better scaling of the SCIT volumes and association with NLDN flash data. More robust methods of spacial clustering and temporal correlation of detected cells allows the tracking of a much more complex cellular structure during the March 15<sup>th</sup> events.

Normalization of flash rates by cell size allowed inter-comparison of the rates for several different tornadic and non-tornadic cells. The flash rates determined highlight the difficulty in determining a single simple lightning change parameter for all sizes and types of cells. While most tornadic cells show a flash rate jump, usually in CC and/or positive flashes, prior to touchdown, there were significant differences that may be due to cell morphology and size. All of the tornadic cells showed local decreases in flash

rates, primarily for CC and positive flashes, during the periods that the tornadoes were reported on the ground.

Additional research is planned to investigate both a larger number of tornadic and non-tornadic cells, as well as to look at the effects of varying some of the control parameters in the DBSCAN algorithm.

## 6 REFERENCES

- Lakshmanan, V., A. Fritz, T. Smith, K. Hondl, and G. Stumpf (2007), An Automated Technique to Quality Control Radar Reflectivity Data, *Journal of Applied Meteorology and Climatology*, 46(3), 288-305.
- Lakshmanan, V., T. Smith, G. Stumpf, and K. Hondl (2007), The Warning Decision Support System–Integrated Information, *Weather and Forecasting*, 22(3), 596-612.
- Matthews, J. L., and J. Trostel (2010), An Improved Storm Cell Identification and Tracking (SCIT) Algorithm based on DBSCAN Clustering and JPDA Tracking Methods, American Meteorological Society, Atlanta, GA. [online] Available from: [http://ams.confex.com/ams/90annual/techprogram/paper\\_164442.htm](http://ams.confex.com/ams/90annual/techprogram/paper_164442.htm)
- Schultz, C. J., W. A. Petersen, and L. D. Carey (2009), Preliminary Development and Evaluation of Lightning Jump Algorithms for the Real-Time Detection of Severe Weather, *Journal of Applied Meteorology and Climatology*, 48(12), 2543-2563.
- Trostel, J. (2008), P9.14 An examination of radar and lightning characteristics of the “Atlanta Tornado” of March 14-15, 2008, American Meteorological Society, Savannah, GA. [online] Available from: [http://ams.confex.com/ams/24SLS/techprogram/paper\\_142040.htm](http://ams.confex.com/ams/24SLS/techprogram/paper_142040.htm)
- Williams, E., B. Boldi, A. Matlin, M. Weber, S. Hodanish, D. Sharp, S. Goodman, R. Raghavan, and D. Buechler (1999), The behavior of total lightning activity in severe Florida thunderstorms, *Atmospheric Research*, 51(3-4), 245-265, doi:10.1016/S0169-8095(99)00011-3.